27 July 1999

A coupled channel analysis of the centrally produced K^+K^- and $\pi^+\pi^-$ final states in pp interactions at 450 GeV/c

The WA102 Collaboration

D. Barberis[4], F.G. Binon[6], F.E. Close[3,4], K.M. Danielsen[11], S.V. Donskov[5], B.C. Earl[3], D. Evans[3], B.R. French[4], T. Hino[12], S. Inaba[8], A. Jacholkowski[4], T. Jacobsen[11], G.V. Khaustov[5], J.B. Kinson[3], A. Kirk[3], A.A. Kondashov[5], A.A. Lednev[5], V. Lenti[4], I. Minashvili[7], J.P. Peigneux[1], V. Romanovsky[7], N. Russakovich[7], A. Semenov[7], P.M. Shagin[5], H. Shimizu[10], A.V. Singovsky[1,5], A. Sobol[5], M. Stassinaki[2], J.P. Stroot[6], K. Takamatsu[9], T. Tsuru[8], O. Villalobos Baillie[3], M.F. Votruba[3]. Y. Yasu[8].

Abstract

A coupled channel analysis of the centrally produced K^+K^- and $\pi^+\pi^-$ final states has been performed in pp collisions at an incident beam momentum of 450 GeV/c. The pole positions and branching ratios to $\pi\pi$ and $K\overline{K}$ of the $f_0(980)$, $f_0(1370)$, $f_0(1500)$ and $f_0(1710)$ have been determined. A systematic study of the production properties of all the resonances observed in the $\pi^+\pi^-$ and K^+K^- channels has been performed.

Submitted to Physics Letters

1 LAPP-IN2P3, Annecy, France.
2 Athens University, Physics Department, Athens, Greece.
3 School of Physics and Astronomy, University of Birmingham, Birmingham, U.K.
4 CERN - European Organization for Nuclear Research, Geneva, Switzerland.
5 IHEP, Protvino, Russia.
6 IISN, Belgium.
7 JINR, Dubna, Russia.
8 High Energy Accelerator Research Organization (KEK), Tsukuba, Ibaraki 305-0801, Japan.
9 Faculty of Engineering, Miyazaki University, Miyazaki 889-2192, Japan.
10 RCNP, Osaka University, Ibaraki, Osaka 567-0047, Japan.
11 Oslo University, Oslo, Norway.
12 Faculty of Science, Tohoku University, Aoba-ku, Sendai 980-8577, Japan.

Recently the WA102 collaboration has published the results of partial wave analyses of the centrally produced K^+K^- , $K^0_SK^0_S$ [1], $\pi^+\pi^-$ [2] and $\pi^0\pi^0$ [3] channels. A striking feature of these analyses was the result that the $f_J(1710)$ has J = 0 (we shall refer to it as the $f_0(1710)$ hereafter). In these papers the S-wave from each channel was fitted independently using interfering Breit-Wigners and a background. In this present paper we will first show how the resulting parameters change if a different method of fitting is used, namely, a T-Matrix analysis and a K-Matrix analysis using the methods described in ref. [4]. Next we will perform a coupled channel fit to the K^+K^- and $\pi^+\pi^-$ final states in order to determine the pole positions and branching ratios of the observed mesons. Finally we will present information on the production kinematics of these resonances.

In our previous publication a fit has been performed to the $\pi^+\pi^-$ S-wave using a coherent sum of relativistic Breit-Wigner functions and a background of the form:

$$A(M_{\pi\pi}) = Bgd(M_{\pi\pi}) + \sum_{n=1}^{N_{res}} a_n e^{i\theta_n} BW_n(M_{\pi\pi})$$

where the background has been parameterised as

$$Bgd(M_{\pi\pi}) = \alpha(M_{\pi\pi} - 2m_\pi)^\beta e^{-\gamma M_{\pi\pi} - \delta M^2_{\pi\pi}}$$

where a_n and θ_n are the amplitude and the phase of the n-th resonance respectively, α, β, γ and δ are real parameters, $BW(M_{\pi\pi})$ is the relativistic Breit-Wigner function for a spin zero resonance. In order to describe the centrally produced $\pi^+\pi^-$ mass spectrum the function $|A(M_{\pi\pi})|^2$ has been multiplied by the kinematical factor $(M_{\pi\pi} - 4m^2_\pi)^{1/2}/M^3_{\pi\pi}$ [5]. The resulting function is then convoluted with a Gaussian to account for the experimental mass resolution.

In this present paper we use the Flatté formula [6] to describe the $f_0(980)$, this is referred to as Method I. For the $\pi^+\pi^-$ channel the Breit-Wigner has the form:

$$BW(M_{\pi\pi}) = \frac{m_0\sqrt{\Gamma_i}\sqrt{\Gamma_\pi}}{m_0^2 - m^2 - im_0(\Gamma_\pi + \Gamma_K)}$$

and in the K^+K^- channel the Breit-Wigner has the form:

$$BW(M_{KK}) = \frac{m_0\sqrt{\Gamma_i}\sqrt{\Gamma_K}}{m_0^2 - m^2 - im_0(\Gamma_\pi + \Gamma_K)}$$

where Γ_i is absorbed into the intensity of the resonance. Γ_π and Γ_K describe the partial widths of the resonance to decay to $\pi\pi$ and $K\overline{K}$ and are given by

$$\Gamma_\pi = g_\pi(m^2/4 - m^2_\pi)^{1/2}$$

$$\Gamma_K = g_k/2[(m^2/4 - m^2_{K^+})^{1/2} + (m^2/4 - m^2_{K^0})^{1/2}]$$

where g_π and g_K are the squares of the coupling constants of the resonance to the $\pi\pi$ and $K\overline{K}$ systems. The resulting fit is shown in fig. 1a) for the entire mass spectrum and in fig. 1b) for masses above 1 GeV. The sheet II pole positions [7] for the resonances are

$f_0(980)$	M $= (\ 983 \pm\ 8)$	$-i\,(\ 58 \pm 11)$	MeV
$f_0(1370)$	M $= (1306 \pm 18)$	$-i\,(111 \pm 23)$	MeV
$f_0(1500)$	M $= (1502 \pm 12)$	$-i\,(\ 65 \pm 12)$	MeV
$f_0(1710)$	M $= (1748 \pm 22)$	$-i\,(\ 73 \pm 22)$	MeV

These parameters are consistent with the PDG [8] values for these resonances.

To test the sensitivity of these results on the fitting method used we have also performed a fit to the $\pi^+\pi^-$ mass spectrum using the T-Matrix parameterisation of Zou and Bugg [4]. The invariant amplitude for $\pi^+\pi^-$ central production can be expressed as

$$A = \alpha_1(s)T_{11} + \alpha_2(s)T_{21} \tag{1}$$

where T_{11} and T_{21} are the invariant amplitudes for elastic $\pi\pi \to \pi\pi$ and $K\overline{K} \to \pi\pi$ scattering and are parameterised by

$$T_{11} = \frac{e^{2i\phi}-1}{2i\rho_1} + \frac{g_1 e^{2i\phi}}{M_R^2 - s - i(\rho_1 g_1 + \rho_2 g_2)} \tag{2}$$

$$T_{21} = \frac{\sqrt{g_1 g_2}e^{i\phi}}{M_R^2 - s - i(\rho_1 g_1 + \rho_2 g_2)} \tag{3}$$

where $\rho_1 = (1 - 4m_\pi^2/s)^{1/2}$ and $\rho_2 = (1 - 4m_K^2/s)^{1/2}$ are phase space factors and s is the invariant mass squared of the $\pi^+\pi^-$ channel. The background term is presumed to be coupled only to the $\pi\pi$ channel and has the form

$$T_b = \frac{e^{2i\phi}-1}{2i\rho_1} = \frac{1}{A(s) - i\rho_1}$$

which satisfies the unitarity condition. $A(s)$ is an arbitrary real function which has been taken to be of the form

$$A(s) = \frac{1 + a_1 s + a_2 s^2}{b_1(s - m_\pi^2/2) + b_2 s^2}$$

The real functions $\alpha_i(s)$ in equation (1) describe the coupling of the initial state to the channel i. These functions are approximated by the power expression [5]:

$$\alpha_i(s) = \sum_{n=0} \alpha_i^n \{\frac{s}{4m_K^2}\}^n$$

where the factor $4m_K^2$ is introduced as a convenient scaling. It has been found that $n = 3$ is sufficient to describe the S-wave distribution.

In order to describe the centrally produced $\pi^+\pi^-$ mass spectrum, the function $|A(M_{\pi\pi})|^2$ has been multiplied by the kinematical factor $(M_{\pi\pi} - 4m_\pi^2)^{1/2}/M_{\pi\pi}^3$ [5] and the resulting function is then convoluted with a Gaussian to account for the experimental mass resolution. The resulting fit is shown in fig. 1c) for the entire mass spectrum and in fig. 1d) for masses above 1 GeV. As can be seen the fit does not describe well the region above 1.0 GeV. The sheet II pole corresponding to the $f_0(980)$ is

$$M = (993 \pm 8) - i(38 \pm 9) \quad \text{MeV}$$

There are two poles from the background term with

$$M_1 = (388 \pm 55) - i(223 \pm 28) \quad \text{MeV}$$
$$M_2 = (1541 \pm 32) - i(143 \pm 21) \quad \text{MeV}$$

The first pole may be associated with the low mass S-wave. The NA12/2 collaboration [9] have previously shown that this region may be interpreted as being due to the σ particle. The second pole would appear to be in the region of the $f_0(1500)$ but the width is very broad. This is due to the fact that the fit is not able to properly describe the region around 1.3 GeV.

Adding one more term to equations (2) and (3) to describe the 1300 MeV mass region improves the fit considerably but still does not describe the region around 1700 MeV. In order to produce a satisfactory fit two terms have to be added to equations (2) and (3) to account for the $f_0(1370)$ and $f_0(1710)$ which results in the fit shown in fig. 1e) for masses above 1 GeV. The new sheet II pole positions are

$$
\begin{array}{llll}
f_0(980) & \mathrm{M} & = (\ 992 \pm 6) - i(\ 52 \pm 9) & \mathrm{MeV} \\
f_0(1370) & \mathrm{M} & = (1310 \pm 30) - i(134 \pm 23) & \mathrm{MeV} \\
f_0(1500) & \mathrm{M} & = (1497 \pm 17) - i(\ 82 \pm 21) & \mathrm{MeV} \\
f_0(1710) & \mathrm{M} & = (1752 \pm 15) - i(\ 53 \pm 12) & \mathrm{MeV}
\end{array}
$$

These parameters are consistent with the values from the fit using interfering Breit-Wigners and with the PDG [8] values for these resonances.

An alternative parameterisation is to use the K-Matrix formalism. In this case the Lorentz invariant T-Matrix is expressed as

$$\hat{T} = \hat{K}(1 - i\hat{\rho}\hat{K})^{-1}$$

where for the case of $\pi\pi$ and $K\overline{K}$ final states $\hat{\rho}$ is a 2 dimensional diagonal matrix and $\hat{K}$ is a real symmetric 2 dimensional matrix of the form

$$K_{ij} = \frac{a_i a_j}{M_R^2 - s} + \frac{b_i b_j}{s_b - s} + \gamma_{ij}$$

In the K-Matrix formalism the background is assumed to couple to both the $\pi\pi$ and $K\overline{K}$ channels. In order to describe the centrally produced $\pi^+\pi^-$ mass spectrum, the function $|A(M_{\pi\pi})|^2$ has been multiplied by the kinematical factor $(M_{\pi\pi} - 4m_\pi^2)^{1/2}/M_{\pi\pi}^3$ [5] and the resulting function is then convoluted with a Gaussian to account for the experimental mass resolution.

Two coupled channel resonances are found from the fit shown in fig. 1f) for the entire mass spectrum and in fig. 1g) for masses above 1 GeV with their sheet II T-Matrix poles at

$$
\begin{array}{lll}
M_1 & = (\ 988 \pm 18) - i(\ 39 \pm 12) & \mathrm{MeV} \\
M_2 & = (1526 \pm 22) - i(191 \pm 53) & \mathrm{MeV}
\end{array}
$$

As in the case of the T-Matrix analysis the fit fails in the 1.3 GeV region. Adding one additional pole improves the fit. However, in order to to obtain a satisfactory fit it is found necessary to include two extra poles. The fit shown is in fig. 1h) for masses above 1 GeV and results in sheet II pole positions of

$$
\begin{array}{llll}
f_0(980) & \mathrm{M} & = (\ 982 \pm 9) - i(\ 38 \pm 16) & \mathrm{MeV} \\
f_0(1370) & \mathrm{M} & = (1290 \pm 30) - i(104 \pm 25) & \mathrm{MeV} \\
f_0(1500) & \mathrm{M} & = (1510 \pm 10) - i(\ 56 \pm 15) & \mathrm{MeV} \\
f_0(1710) & \mathrm{M} & = (1709 \pm 15) - i(\ 75 \pm 18) & \mathrm{MeV}
\end{array}
$$

These parameters are consistent with the values from the two previous fits.

Finally, in order to perform a coupled channel fit to the $\pi^+\pi^-$ and K^+K^- final states a correct normalisation of the two data sets has to be performed. The fit has been modified to take into account the relative differences in geometrical acceptance, event reconstruction and event selection. The fit also includes corrections for the unseen decay modes so that the branching ratio $\pi\pi$ to $K\overline{K}$ can be calculated. In addition to the resonances discussed above, the $a_0(980)$ can also contribute to the $K\overline{K}$ S-wave mass spectrum. The contribution from $a_0(980) \to K^+K^-$ has been calculated from the observed decay $a_0(980) \to \eta\pi$ and the measured branching ratio of the $a_0(980)$ [10]. The calculated contribution (500 $\pm$ 120 events) has been included in the fit as a histogram. There is no evidence for any $a_0(1450)$ contribution in the $\eta\pi$ channel and hence it has not been included in the fit to the $K\overline{K}$ S-wave.

The coupled channel fit has been performed using the three methods described above. The following pole positions and branching ratios quoted for the resonances are a mean from the three methods. The statistical error is the largest error from the three fits and the systematic error quoted represents the spread of the values from the three methods. The results of the combined fit are shown in fig. 2. The sheet II pole positions are

$$
\begin{array}{llll}
f_0(980) & \mathrm{M} & = (\ 987 \pm\ 6 \pm\ 6)\ -i\,(\ 48 \pm 12 \pm 8) & \mathrm{MeV} \\
f_0(1370) & \mathrm{M} & = (1312 \pm 25 \pm 10)\ -i\,(109 \pm 22 \pm 15) & \mathrm{MeV} \\
f_0(1500) & \mathrm{M} & = (1502 \pm 12 \pm 10)\ -i\,(\ 49 \pm\ 9 \pm 8) & \mathrm{MeV} \\
f_0(1710) & \mathrm{M} & = (1727 \pm 12 \pm 11)\ -i\,(\ 63 \pm\ 8 \pm 9) & \mathrm{MeV}
\end{array}
$$

These parameters are consistent with the PDG [8] values for these resonances. For the $f_0(980)$ the couplings were determined to be g_π = 0.19 $\pm$ 0.03 $\pm$ 0.04 and g_K =0.40 $\pm$ 0.04 $\pm$ 0.04.

The branching ratios for the $f_0(1370)$, $f_0(1500)$ and $f_0(1710)$ have been calculated to be:

$$\frac{f_0(1370) \to K\overline{K}}{f_0(1370) \to \pi\pi} = 0.46 \pm 0.15 \pm 0.11$$

$$\frac{f_0(1500) \to K\overline{K}}{f_0(1500) \to \pi\pi} = 0.33 \pm 0.03 \pm 0.07$$

$$\frac{f_0(1710) \to K\overline{K}}{f_0(1710) \to \pi\pi} = 5.0 \pm 0.6 \pm 0.9$$

These values are to be compared with the PDG [8] values of 1.35 $\pm$ 0.68 for the $f_0(1370)$ and 0.19 $\pm$ 0.07 for the $f_0(1500)$, which comes from the Crystal Barrel experiment [11]. The value for the $f_0(1710)$ is consistent with the value of 2.56 $\pm$ 0.9 which comes from the WA76 experiment which assumed J = 2 for the $f_J(1710)$ [12].

In our previous publications a study has been performed of resonance production rate as a function of the difference in the transverse momentum vectors (dP_T) between the particles exchanged from the fast and slow vertices [13, 14]. It has been observed[15] that all the undisputed $q\overline{q}$ states (i.e. η, η', $f_1(1285)$ etc.) are suppressed as dP_T goes to zero, whereas the glueball candidates $f_0(1500)$ and $f_2(1950)$ survive. In order to calculate the contribution of each resonance as a function of dP_T, the partial waves have been fitted in three dP_T intervals with the parameters of the resonances fixed to those obtained from the fits to the total data using method I. As an example of how the mass spectra change as a function of dP_T, fig. 3 shows the $\pi^+\pi^-$ S-wave and D-wave in three dP_T intervals.

The S-wave clearly shows that the region around 1.3 GeV is more enhanced at large dP_T in contrast to the low mass part of the spectrum. This is not due to feed through from the D-wave which has been estimated to be less than 3 % in this mass region. In the D-wave the $f_2(1270)$ is suppressed at small dP_T in contrast to the behaviour of the low mass part of the D-wave.

Table 1 gives the percentage of each resonance in three dP_T intervals together with the ratio of the number of events for $dP_T < 0.2$ GeV to the number of events for $dP_T > 0.5$ GeV for each resonance considered. As can be seen from table 1, the $\rho^0(770)$, $f_2(1270)$ and $f_2'(1525)$ are suppressed at small dP_T in contrast to the $f_0(980)$, $f_0(1500)$ and $f_0(1710)$.

The azimuthal angle (ϕ) is defined as the angle between the p_T vectors of the two protons. In order to determine the ϕ dependence for the resonances observed, the partial waves have been fitted in 30 degree bins of ϕ with the parameters of the resonances fixed to those obtained from the fits to the total data. The fraction of each resonance as a function of ϕ is plotted in fig. 4. The ϕ dependences are clearly not flat and considerable variation is observed between the different resonances.

In order to determine the four momentum transfer dependence (t) of the resonances observed in the $\pi^+\pi^-$ and K^+K^- channels the partial waves have been fitted in 0.1 GeV^2 bins of t with the parameters of the resonances fixed to those obtained from the fits to the total data. Fig. 5 shows the four momentum transfer from one of the proton vertices for these resonances. The distributions for the $f_0(980)$, $f_0(1370)$, $f_0(1500)$, $f_0(1710)$ and $\rho(770)$ have been fitted with a single exponential of the form $exp(-b|t|)$ and the values of b found are given in table 2. The distributions for the $f_2(1270)$ and $f_2'(1525)$ cannot be fitted with a single exponential. Instead they have been fitted to the form

$$\frac{d\sigma}{dt} = \alpha e^{-b_1 t} + \beta t e^{-b_2 t}$$

The parameters resulting from the fit are given in table 3.

In a previous publication by the WA76 collaboration [16] the ratios of the production cross sections for the $\rho(770)$, $f_0(980)$ and $f_2(1270)$ were calculated at $\sqrt{s}$ = 12.7 and 23.8 GeV. However, the experiment at 300 GeV ($\sqrt{s}$ = 23.8 GeV) was only sensitive to ϕ angles less than 90 degrees and the acceptance program that had been used assumed a flat ϕ distribution. Hence the cross sections at 300 GeV were underestimated for the $\rho(770)$ and $f_2(1270)$ and overestimated for the $f_0(980)$.

After correcting for geometrical acceptances, detector efficiencies, losses due to cuts, and unseen decay modes, the ratios of the cross-sections for the $\rho(770)$, $f_0(980)$, $f_2(1270)$ and in addition, the $f_0(1500)$ at $\sqrt{s}$ = 29.1 and 12.7 GeV are given in table 4. The cross sections for the $f_0(980)$, $f_2(1270)$ and $f_0(1500)$ are compatible with being independent of energy which is consistent with them being produced via double Pomeron exchange [17].

In summary, a coupled channel fit has been performed to the centrally produced $\pi^+\pi^-$ and K^+K^- mass spectra. The pole positions and branching ratios of the $f_0(980)$, $f_0(1370)$, $f_0(1500)$

and $f_0(1710)$ have been determined using three different methods which give consistent results. An analysis of the dP_T dependence of the resonances observed shows that the undisputed $q\overline{q}$ mesons are suppressed at small dP_T in contrast to the enigmatic $f_0(980)$, $f_0(1500)$ and $f_0(1710)$. Considerable variation is observed in the ϕ distributions of the produced mesons.

Acknowledgements

This work is supported, in part, by grants from the British Particle Physics and Astronomy Research Council, the British Royal Society, the Ministry of Education, Science, Sports and Culture of Japan (grants no. 04044159 and 07044098), the French Programme International de Cooperation Scientifique (grant no. 576) and the Russian Foundation for Basic Research (grants 96-15-96633 and 98-02-22032).

References

[1] D. Barberis *et al.,* Phys. Lett. **B453** (1999) 305.

[2] D. Barberis *et al.,* Phys. Lett. **B453** (1999) 316.

[3] D. Barberis *et al.,* Phys. Lett. **B453** (1999) 325.

[4] B.S. Zou and D.V. Bugg, Phys. Rev. **D48** (1993) R3948.

[5] K.L. Au, D. Morgan and M.R. Pennington, Phys. Rev. **D35** (1987) 1633.

[6] S.M. Flatté, Phys. Lett. **B38** (1972) 232.

[7] D. Morgan, Phys. Lett. **B51** (1974) 71.

[8] Particle Data Group, European Physical Journal **C3** (1998) 1.

[9] D. Alde *et al.,* Phys. Lett. **B397** (1997) 350.

[10] D. Barberis *et al.,* Phys. Lett. **B440** (1998) 225.

[11] A. Abele *et al.,* Phys. Rev. **D57** (1998) 3860.

[12] T.A. Armstrong *et al.,* Zeit. Phys. **C51** (1991) 351.

[13] D. Barberis *et al.,* Phys. Lett. **B397** (1997) 339.

[14] F.E. Close and A. Kirk, Phys. Lett. **B397** (1997) 333.

[15] A. Kirk, Yad. Fiz. **62** (1999) 439.

[16] T.A. Armstrong *et al.,* Zeit. Phys. **C51** (1991) 351.

[17] S.N. Ganguli and D.P. Roy, Phys. Rep. **67** (1980) 203.

Table 1: Production of the resonances as a function of dP_T expressed as a percentage of their total contribution and the ratio (R) of events produced at $dP_T \leq 0.2$ GeV to the events produced at $dP_T \geq 0.5$ GeV.

	$dP_T \leq 0.2$ GeV	$0.2 \leq dP_T \leq 0.5$ GeV	$dP_T \geq 0.5$ GeV	$R = \frac{dP_T \leq 0.2GeV}{dP_T \geq 0.5GeV}$
$f_0(980)$	23.1 ± 2.2	50.6 ± 2.7	26.2 ± 2.7	0.88 ± 0.12
$f_0(1370)$	18.1 ± 4.0	32.0 ± 2.0	49.9 ± 2.9	0.36 ± 0.08
$f_0(1500)$	23.5 ± 2.5	54.1 ± 5.0	22.3 ± 3.0	1.05 ± 0.18
$f_0(1710)$	26.4 ± 1.2	45.8 ± 1.0	27.8 ± 1.1	0.95 ± 0.06
$\rho(770)$	6.4 ± 2.5	41.1 ± 4.0	52.5 ± 3.0	0.12 ± 0.05
$f_2(1270)$	7.6 ± 1.2	29.5 ± 0.6	62.9 ± 1.7	0.12 ± 0.02
$f_2'(1525)$	4.3 ± 3.0	35.7 ± 3.0	60.0 ± 4.0	0.07 ± 0.04
$f_2(2150)$	2.6 ± 3.0	53.6 ± 3.6	43.6 ± 3.2	0.06 ± 0.08

Table 2: The slope parameter b from a single exponential fit to the $|t|$ distributions.

	$f_0(980)$	$f_0(1370)$	$f_0(1500)$	$f_0(1710)$	$\rho(770)$
b/GeV^{-2}	5.3 ± 0.2	6.7 ± 0.5	5.2 ± 0.5	6.5 ± 0.8	5.8 ± 0.1

Table 3: The slope parameters from a fit to the $|t|$ distributions of the form $\frac{d\sigma}{dt} = \alpha e^{-b_1 t} + \beta t e^{-b_2 t}$.

	α	b_1 GeV^{-2}	β	b_2 GeV^{-2}
$f_2(1270)$	0.25 ± 0.04	8.3 ± 3.0	5.3 ± 1.0	8.7 ± 0.4
$f_2'(1525)$	0.4 ± 0.3	8.3 ± 5.0	5.3 ± 4.0	7.7 ± 3.3

Table 4: The ratio of the cross sections at $\sqrt{s} = 29.1$ and 12.7 GeV.

	$\rho(770)$	$f_0(980)$	$f_2(1270)$	$f_0(1500)$
$\frac{\sigma(\sqrt{s}=29.1)}{\sigma(\sqrt{s}=12.7)}$	0.36 ± 0.05	1.28 ± 0.21	0.98 ± 0.13	1.07 ± 0.14

Figures

Figure 1: The $\pi^+\pi^-$ mass spectrum with a) and b) fit using interfering Breit-Wigners. Fit using the T-Matrix parameterisation c) and d) the original fit and e) including two extra poles. Fit using the K-Matrix parameterisation f) and g) the original fit and h) including another two poles.

Figure 2: A coupled channel fit to the $\pi^+\pi^-$ and K^+K^- S-wave distributions.

Figure 3: The $\pi^+\pi^-$ S-wave and D-wave in three dP_T intervals.

Figure 4: The ϕ distributions of the resonances observed in the $\pi^+\pi^-$ and K^+K^- channels.

Figure 5: The four momentum transfer squared ($|t|$) from one of the proton vertices for the resonances observed in the $\pi^+\pi^-$ and K^+K^- channels.

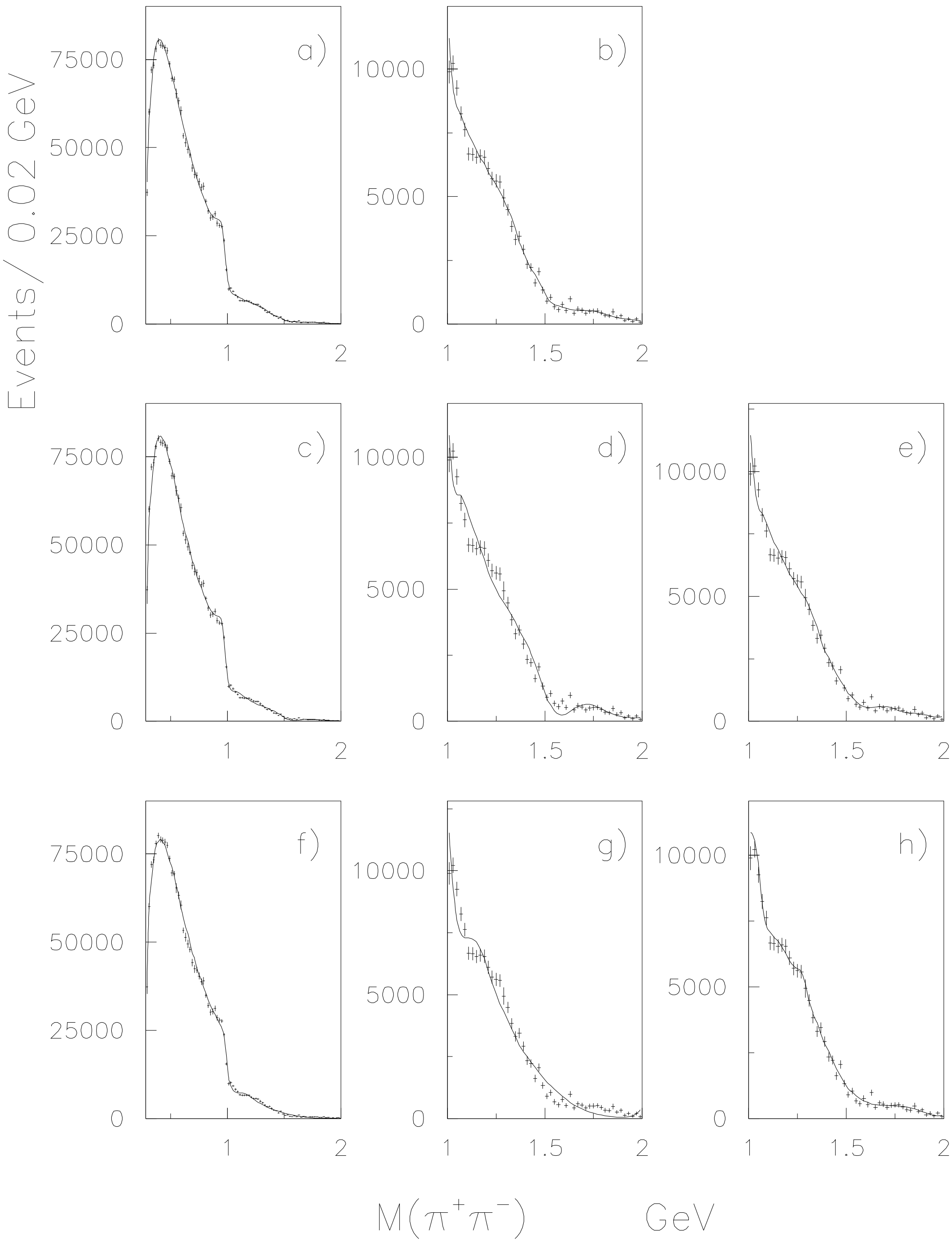

Events/ 0.02 GeV
a)
b)
c)
d)
e)
f)
g)
h)
75000
50000
25000
0
10000
5000
1
1.5
2
$M(\pi^+\pi^-)$ GeV

Figure 1

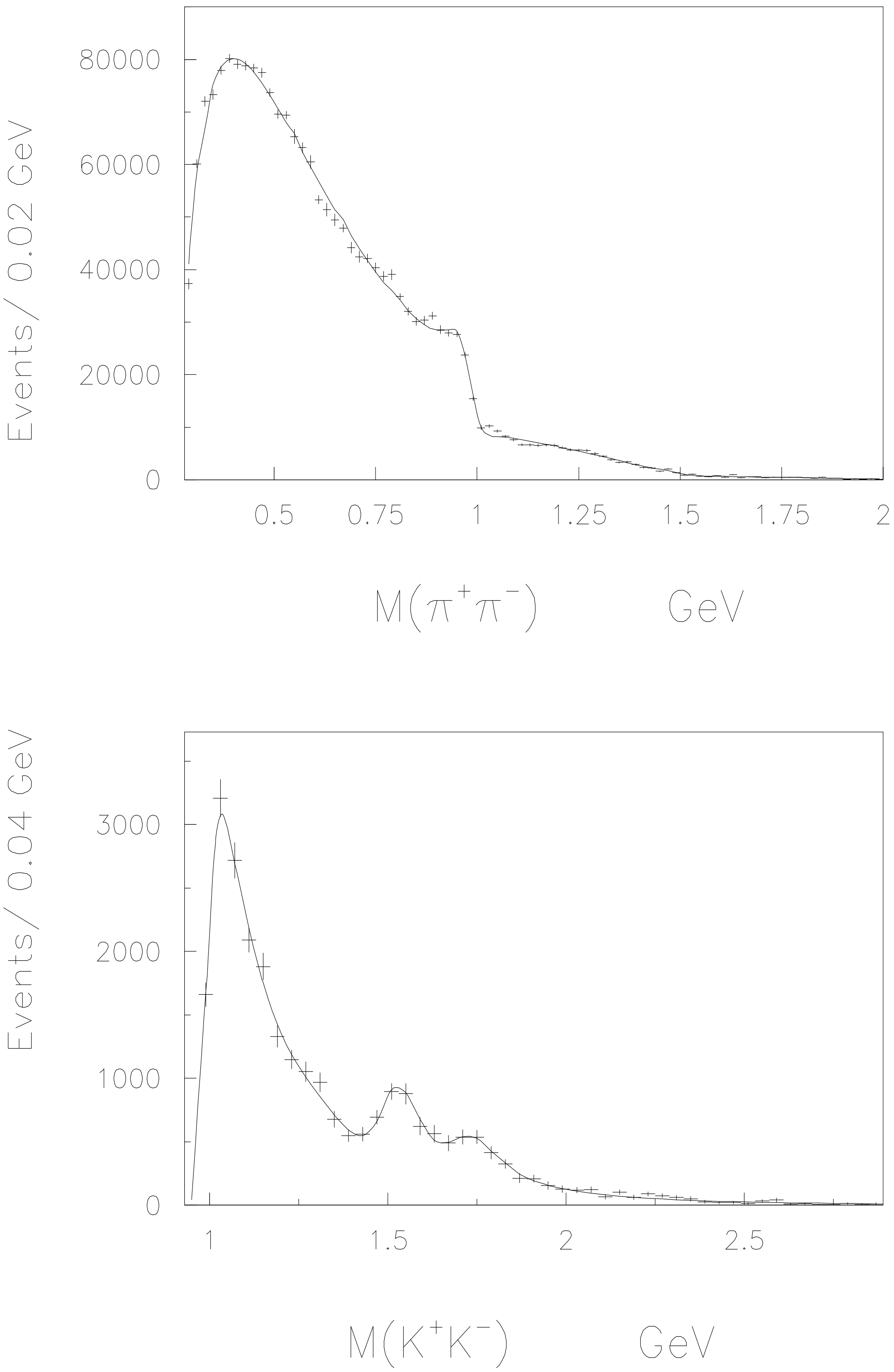

Events/ 0.02 GeV
80000
60000
40000
20000
0
0.5
0.75
1
1.25
1.5
1.75
2
$M(\pi^+\pi^-)$ GeV
Events/ 0.04 GeV
3000
2000
1000
0
1
1.5
2
2.5
$M(K^+K^-)$ GeV

Figure 2

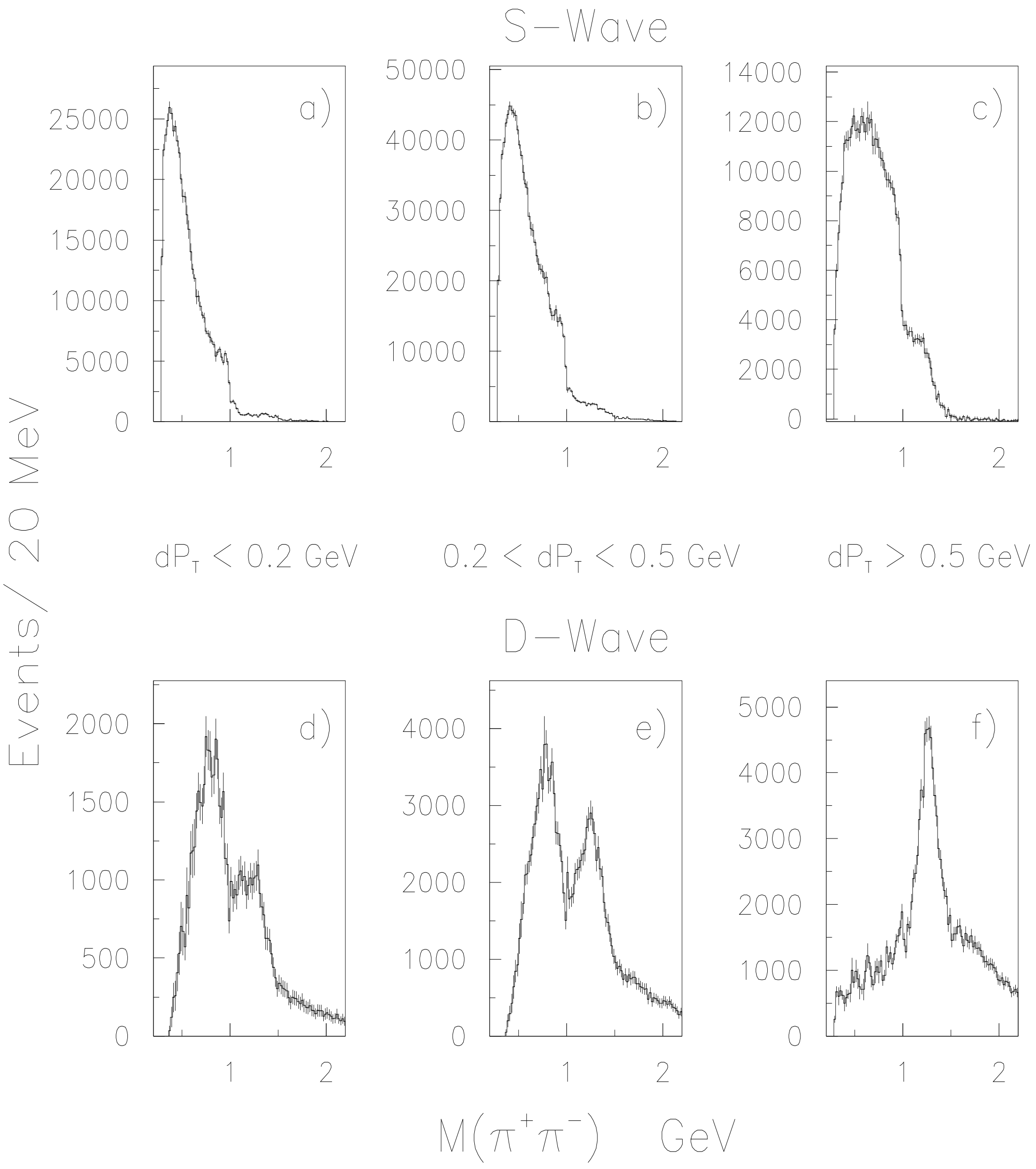

S−Wave
a)
b)
c)
dP_T < 0.2 GeV
0.2 < dP_T < 0.5 GeV
dP_T > 0.5 GeV
D−Wave
d)
e)
f)
Events/ 20 MeV
M(π⁺π⁻) GeV

Figure 3

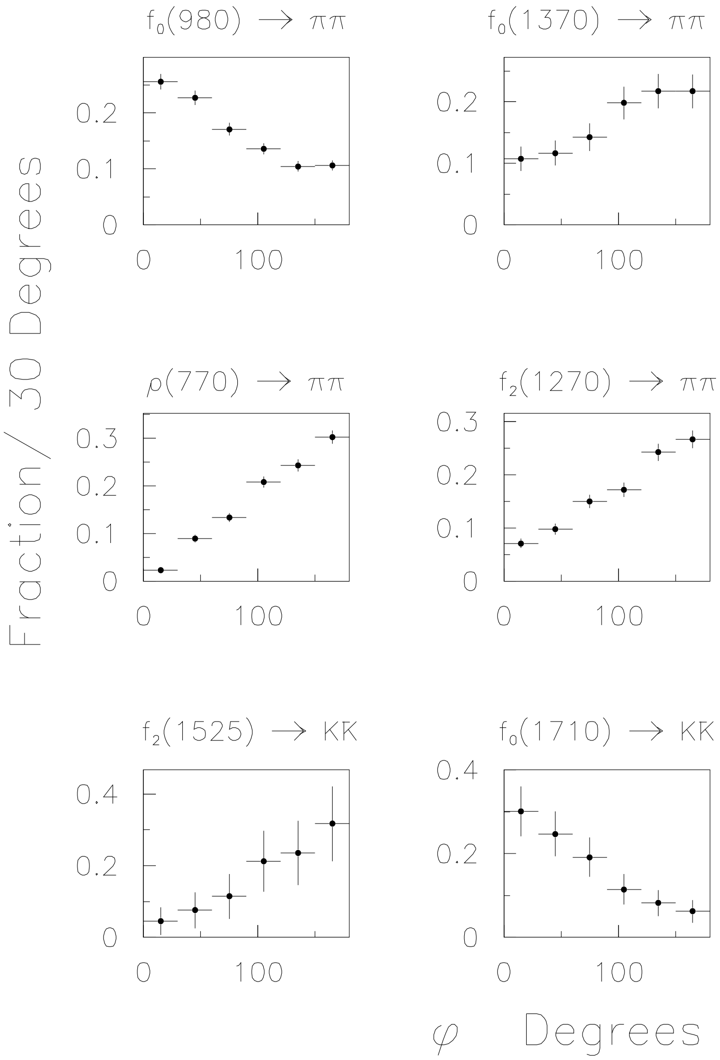

$f_0(980) \to \pi\pi$
$f_0(1370) \to \pi\pi$
$f_0(1500) \to \pi\pi$
$\rho(770) \to \pi\pi$
$f_2(1270) \to \pi\pi$
$f_2(1525) \to K\bar{K}$
$f_0(1710) \to K\bar{K}$
Fraction/ 30 Degrees
φ Degrees

Figure 4

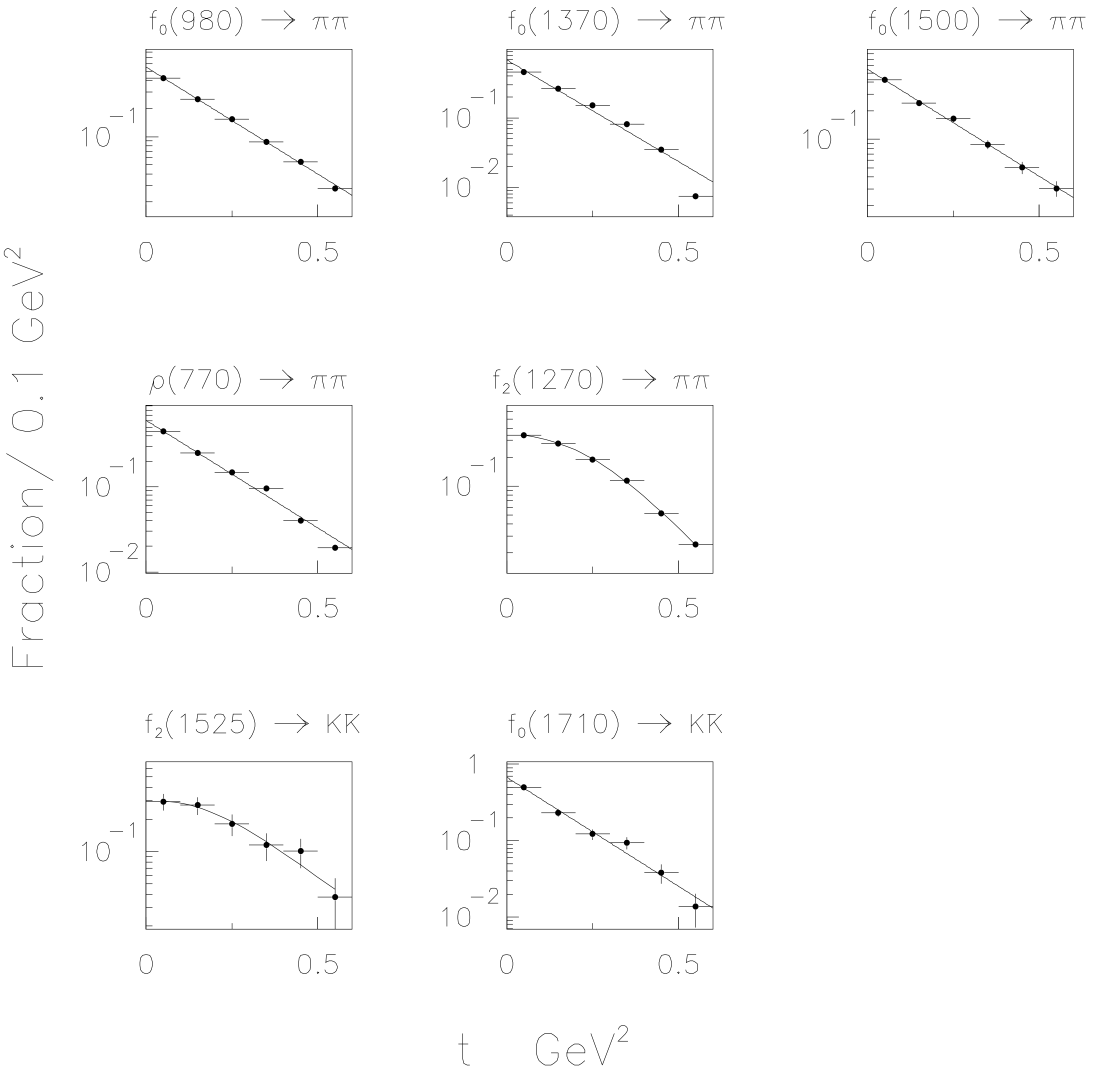
$f_0(980) \rightarrow \pi\pi$
$f_0(1370) \rightarrow \pi\pi$
$f_0(1500) \rightarrow \pi\pi$
$\rho(770) \rightarrow \pi\pi$
$f_2(1270) \rightarrow \pi\pi$
$f_2(1525) \rightarrow K\bar{K}$
$f_0(1710) \rightarrow K\bar{K}$
Fraction/ 0.1 GeV^2
t GeV^2

Figure 5